

Impaired transmissibility of atypical prions from genetic CJD^{G114V}

Ignazio Cali, PhD, Fadi Mikhail, MD, Kefeng Qin, PhD, Crystal Gregory, MS, Ani Solanki, BS, Manuel Camacho Martinez, PhD, Lili Zhao, MS, Brian Appleby, MD, Pierluigi Gambetti, MD, Eric Norstrom, PhD, and James A. Mastrianni, MD, PhD

Correspondence
Dr. Mastrianni
jmastria@uchicago.edu

Neurol Genet 2018;4:e253. doi:10.1212/NXG.0000000000000253

Abstract

Objective

To describe the clinicopathologic, molecular, and transmissible characteristics of genetic prion disease in a young man carrying the *PRNP*-G114V variant.

Methods

We performed genetic, histologic, and molecular studies, combined with in vivo transmission studies and in vitro replication studies, to characterize this genetic prion disease.

Results

A 24-year-old American man of Polish descent developed progressive dementia, aphasia, and ataxia, leading to his death 5 years later. Histologic features included widespread spongiform degeneration, gliosis, and infrequent PrP plaque-like deposits within the cerebellum and putamen, best classifying this as a Creutzfeldt-Jakob disease (CJD) subtype. Molecular typing of proteinase K-resistant PrP (resPrP^{Sc}) revealed a mixture of type 1 (~21 kDa) and type 2 (~19 kDa) conformations with only 2, rather than the usual 3, PrP^{Sc} glycoforms. Brain homogenates from the proband failed to transmit prion disease to transgenic Tg(HuPrP) mice that overexpress human PrP and are typically susceptible to sporadic and genetic forms of CJD. When subjected to protein misfolding cyclic amplification, the PrP^{Sc} type 2 (~19 kDa) was selectively amplified.

Conclusions

The features of genetic CJD^{G114V} suggest that residue 114 within the highly conserved palindromic region (113-AGAAAAGA-120) plays an important role in prion conformation and propagation.

From the Department of Pathology (I.C., M.C.M., P.G.), Case Western University, Cleveland, OH; Department of Neurology (K.Q., F.M., C.G., A.S., L.Z., J.A.M.), University of Chicago; and Department of Biological Sciences (E.N.), DePaul University, Chicago, IL.

Funding information and disclosures are provided at the end of the article. Full disclosure form information provided by the authors is available with the full text of this article at Neurology.org/NG.

The Article Processing Charge was funded by the authors.

This is an open access article distributed under the terms of the Creative Commons Attribution-NonCommercial-NoDerivatives License 4.0 (CC BY-NC-ND), which permits downloading and sharing the work provided it is properly cited. The work cannot be changed in any way or used commercially without permission from the journal.

Glossary

BH = brain homogenate; **CJD** = Creutzfeldt-Jakob disease; **DPBS** = Dulbecco phosphate-buffered saline; **DWI** = diffusion-weighted imaging; **gCJD** = genetic CJD; **GFAP** = glial fibrillary acidic protein; **GSS** = Gerstmann-Sträussler-Scheinker; **IBH** = infectious BH; **IHC** = immunohistochemistry; **MMSE** = Mini-Mental State Examination; **NBH** = normal BH; **PrP^C** = cellular prion protein; **PK** = proteinase K; **PMCA** = protein misfolding cyclic amplification; **PTFE** = polytetrafluoroethylene; **sCJD** = sporadic CJD; **SD** = spongiform degeneration; **WB** = Western blot.

Prion diseases are rare transmissible neurodegenerative disorders that result from the accumulation of a misfolded isoform (PrP^{Sc}) of the cellular prion protein (PrP^C).¹ Several subtypes are recognized based on their clinical, histopathologic, and PrP^{Sc} conformational phenotype.² PrP^{Sc} conformation is approximated by the electrophoretic gel migration pattern of proteinase K (PK)-resistant PrP^{Sc} (resPrP^{Sc}). ResPrP^{Sc} from Creutzfeldt-Jakob disease (CJD) typically displays an unglycosylated fraction that migrates at either ~21 kDa (PrP^{Sc} type 1) or ~19 kDa (PrP^{Sc} type 2),³ along with 2 higher molecular weight monoglycosylated and diglycosylated PrP^{Sc} fractions. Experimental transmission of sporadic CJD (sCJD) and genetic CJD (gCJD) to transgenic (Tg) mice that express human (Hu) PrP^C has been useful to prove transmissibility.^{4,5} The in vitro protein misfolding cyclic amplification (PMCA) assay has also been used to assess transmission barriers and the propagation of PrP^{Sc} conformational subtypes between PrP species.^{6,7}

Approximately 10% of prion diseases result from an autosomal dominant sequence change within the coding segment of the *PRNP* gene.² A single nucleotide change within codon 114, resulting in a valine (V) substitution of glycine (G), has been reported in a family from China⁸ and Uruguay.⁹ We report an American case and his father. Several features of gCJD^{G114V}, including an early onset with possible incomplete penetrance, an atypical glycosylation pattern of PrP^{Sc} and, most strikingly, poor transmissibility to Tg(HuPrP) mice, all of which underscore a key role for residue 114 in prion conformation and propagation.

Methods

Histopathology

Histopathology and immunohistochemistry (IHC) of formalin-fixed, formic acid-treated brain tissue were performed, as described previously.¹⁰ Hematoxylin and eosin staining was performed on 5- μ m sections, whereas IHC to PrP and glial fibrillary acidic protein (GFAP) was performed on 8- μ m sections. Each section was deparaffinized, rehydrated, and immersed in tris-buffered saline with Tween 20 before incubation with the EnVision Flex Peroxidase Blocking Reagent (Dako). For PrP immunostaining, sections were incubated with hydrochloric acid (1.5 mmol/L) and microwaved for 15 minutes, probed with monoclonal antibodies (mAb) 3F4 (1:1,000)¹¹ or GFAP (1:20,000) (Sigma-Aldrich) for 60 minutes, and then washed and incubated with Envision Flex/

horseradish polymerase polymer for 30 minutes (Dako) before visualization of the immunoreactivity with Envision Flex 3,3'-diaminobenzidine tetrahydrochloride (Dako).

Molecular studies

Western blot (WB) analysis was performed as previously described.¹⁰ Briefly, a 10% (wt/vol) brain homogenate (BH) was prepared in lysis buffer (100 mM NaCl, 10 mM EDTA, 0.5% NP-40, 0.5% sodium deoxycholate, 10 mM Tris, pH 7.4) or in lysis buffer with 100 mM Tris (100 mM NaCl, 10 mM EDTA, 0.5% NP-40, 0.5% sodium deoxycholate, 100 mM Tris, pH 8.0) and incubated for 1 hour at 37°C with 20 or 100 μ g/mL of PK (Sigma-Aldrich), followed by termination of the reaction with 2 mM phenylmethylsulfonyl fluoride (Sigma-Aldrich). Samples were then diluted 1:1 with 2X Laemmli sample buffer (Bio-Rad) and denatured at 100°C for 10 minutes prior loading onto 12%, 14%, or 15% polyacrylamide gels. For experiments with PMCA, aliquots of “PMCA+” and “PMCA-” (see below) were incubated with either 100 or 50 μ g/ml PK, depending on whether Tg(HuPrP) or Tg(HuPrP^{GlyKO}) was used as the substrate. Incubation with PK was performed at 40°C for 60 minutes with shaking. After denaturation (at 100°C for 10 minutes), samples were precipitated with prechilled methanol (1:10 dilution) sonicated, and loaded onto a 15% Tris-Glycine precast gel (Bio-Rad). Proteins were transferred to polyvinylidene difluoride membranes, probed with mAb 3F4 for 2 hours at 1:40,000 dilution¹² followed by incubation with a horseradish peroxidase-conjugated goat antimouse secondary Ab for 1 hour at 1:3,000 dilution. After incubation with a chemiluminescence substrate (Pierce or Amersham Biosciences), signal was recorded with a Bio-Rad XRS digital document imager or visualized on Kodak films.

Protein misfolding cyclic amplification

BH from 2 distinct Tg mouse models were used as the substrate in PMCA. Tg(HuPrP) mice are hemizygous for human PrP^C, which expresses PrP^C with methionine (M) at codon 129 (i.e., PrP^C-129M) on a PrP^C null background (PrP^{-/-}), at ~8 \times normal level of PrP^C.¹³ The TgNN6h line, hereafter designated Tg(HuPrP^{GlyKO}), expresses human PrP^C with 2 point mutations that eliminate 2 N-linked glycosylation sites on human PrP^C (codons 181 and 197), in which asparagine (N) is replaced by glutamine (Q) (PrP-N181Q/N197Q).¹⁴ These mice are homozygous for the transgene that is expressed at ~0.6-fold that of normal mouse brain PrP levels. Brains harvested from 1.5-month-old healthy Tg mice were perfused with 5 mM EDTA in 1X Dulbecco phosphate-buffered

saline (1X DPBS). Ten percent normal BH was prepared in conversion buffer (150 mM NaCl, 1% Triton X-100, 1X Protease Inhibitor Cocktail in 1X DPBS) and centrifuged at $800 \times g$ at 4°C for 1 minute. The collected supernatants (hereafter designated as NBH) were used as the “substrate” for the PMCA reaction. BH from the frontal cortex of the proband, used as “seed” (hereafter identified as infectious BH or IBH), was prepared following the same procedure used to generate the NBH.

PMCA was performed as previously described with few modifications.¹⁵ The NBH from Tg(HuPrP) or Tg(HuPrP^{GlyKO}) and IBH from the proband or control cases of sCJD were mixed in a 9:1 ratio in a test tube, in the presence of 0.05% digitonin detergent (Sigma-Aldrich) and one 2.38 mm-diameter polytetrafluoroethylene bead (McMaster-Carr). One aliquot of the NBH-IBH mixture was subjected to PMCA (PMCA+), and one aliquot was stored at -80°C and used as the negative control (PMCA-). PMCA reactions were carried out in a programmable sonicator (Misonix Sonicator S-4000; Misonix Inc, Farmingdale, NY) for a total of 96 cycles of sonication. Each cycle consisted of 30 seconds of sonication (Amplitude 98, wattage 230–250) and 29.5 minutes of incubation at 37°C.

Standard protocol approvals, registrations, and patient consents

Human-related studies were conducted under an approved University of Chicago Institutional Review Board protocol (#9713), and animal studies were performed under an approved University of Chicago Institutional Animal Care and Use Committee approval of protocol (#70735).

PRNP gene analysis

DNA was extracted from whole blood, and the entire coding segment of the *PRNP* gene was amplified by PCR using previously reported primers¹⁰ and bidirectional sequencing using an automated sequencer.

Prion transmissions

Fresh-frozen brain from the frontal cortex was homogenized in 1X phosphate buffered saline to a final concentration of 1%, as previously described.¹⁶ Tg mice expressing human PrP^C with Met coding at residue 129 on a mouse PrP knock-out background (i.e., Tg[*HuPrP*-129M]*Prnp*^{0/0}) were previously constructed and described elsewhere.¹³ Mice were anesthetized with a xylazine/ketamine mixture, the head fixed in a small animal stereotaxic instrument (Kopf) and intracerebrally inoculated with BH, directly through the scalp, as described previously.¹³ Typical symptoms of prion disease in mice, including reduced spontaneous movement, scruffy coat, hunched back, and progressively unsteady gait, were monitored every other day. When symptomatic and near-terminal, mice were killed and their brains harvested, freshly hemisectioned, half frozen in dry ice, and half fixed in 2% formalin. All mouse studies were approved by the Institutional Animal Care and Use Committee before study.

Results

Case report

A 24-year-old right-handed white man with no known medical history except for a mild learning disability developed general and episodic anxiety, intermittent confusion, fatigue, memory impairment, and slurred speech ~1 year before seeking medical attention. Initial neurologic evaluation demonstrated mild hypomimia, finger agnosia, and fine bilateral hand tremor. A neuropsychological battery revealed a full-scale IQ of 73, impaired attention, concentration, memory, and mild-to-moderate executive dysfunction. An EEG showed paroxysmal diffuse 4–5 Hz slow activity, with occasional sharp wave-like morphology. An extensive workup included routine laboratory tests for dementia, in addition to antithyroid antibodies, a paraneoplastic panel that included NMDA and GAD65 antibodies, amino acid profile, and heavy metal testing, all of which were negative. CSF cell count, glucose, protein, angiotensin converting enzyme level, VDRL, Lyme PCR, total tau, phosphorylated tau, Aβ42, and 14-3-3 protein were within normal range or negative, as was bacterial, acid-fast bacilli, and fungal cultures. Brain MRI was reported as normal.

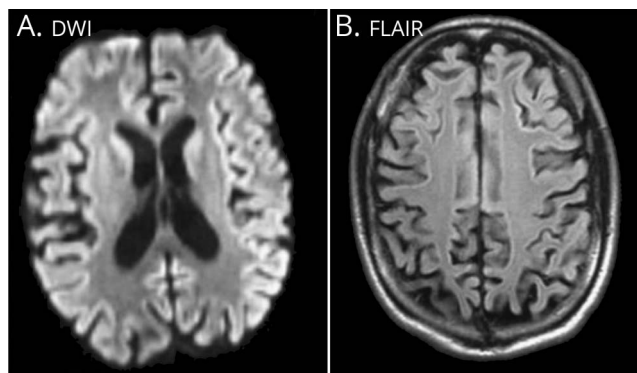
Over the next year, he became more withdrawn, declined cognitively, developed progressive clumsiness, prominent word-finding difficulty, and slowed motor skills that led to 3 car accidents. At the time, he had a coarse hand and head tremor, cogwheel rigidity of the limbs, stooped posture, and a mildly spastic gait with impaired arm swing. He scored 20 of 30 on the Mini-Mental State Examination.¹⁷ Fluorodeoxyglucose PET exhibited decreased but symmetric cortical metabolism, more pronounced in the posterior parietal, temporal, and occipital regions, while thalamic uptake was similar to the cortex, and there was a relative increase in metabolic activity in the basal ganglia. Diffusion-weighted imaging (DWI) sequences on MRI displayed restricted diffusion throughout the cortical ribbon, and right, greater than left, cortical atrophy (figure 1, A and B). Over the next 2 years, the patient developed global aphasia, choreiform movements and myoclonus of the upper extremities, increased axial rigidity, and severe gait ataxia, ultimately confining him to a wheelchair and eventual death 5 years from the initial onset of symptoms, at age 29 years.

The proband’s father suffered a similar course, beginning at age 32 years, with progressive cognitive decline and prominent aphasia that progressed to mutism, in addition to visual hallucinations, gait ataxia, postural instability, and generalized myoclonus. The brain MRI report noted “diffuse cerebral atrophy, markedly out of proportion for age,” but films were not available for review. He died at age 34 and underwent brain autopsy, although *PRNP* gene sequencing was not performed at the time. Tissue was unavailable for genetic testing, but limited fixed tissue was available for histologic staining.

Pathologic studies

Widespread spongiform degeneration (SD) and gliosis were most severe in the frontal (figure 2A), temporal, and parietal

Figure 1 Brain MRI of the gCJD^{G114V} proband during the 3rd year of his disease



(A) DWI sequence shows restricted diffusion throughout the cortical ribbon and within the caudate nuclei. (B) FLAIR sequence shows diffuse cortical atrophy. DWI = diffusion-weighted imaging; FLAIR = fluid-attenuated inversion recovery.

cortices, and least severe in the occipital lobe and hippocampus (figure 2, B and C). Severe SD was also present within the putamen (figure 2D), but not the adjacent globus pallidus, and within the medial nuclei of the thalamus, but not the lateral thalamus (not shown). The midbrain, cerebellum (figure 2, E and F), pons, and medulla were also devoid of SD

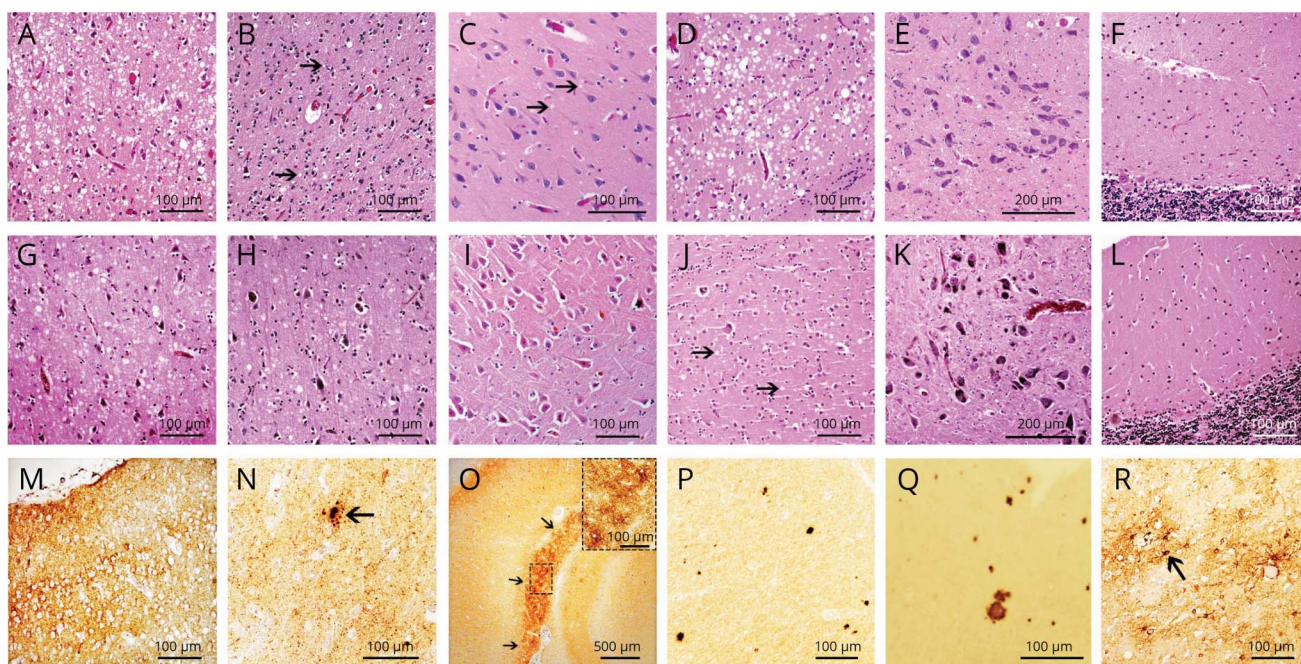
(not shown). IHC with anti-PrP mAb 3F4 revealed fine, diffuse PrP staining and occasionally larger granules within the cerebral cortex (figure 2, M–O) and neostriatum (figure 2P), as well as plaque-like PrP deposits in the putamen and cerebellum (figure 2, P and Q). IHC for GFAP in frontal and temporal lobes revealed intense reactive astrogliosis (figure 2R).

In a limited number of sections from the proband's father, SD was observed within the cerebral cortex and putamen (figure 2, G, H, and J), with sparing of the hippocampus, midbrain, pons, medulla, and cerebellum (figure 2, I, K, and L).

Genetic studies

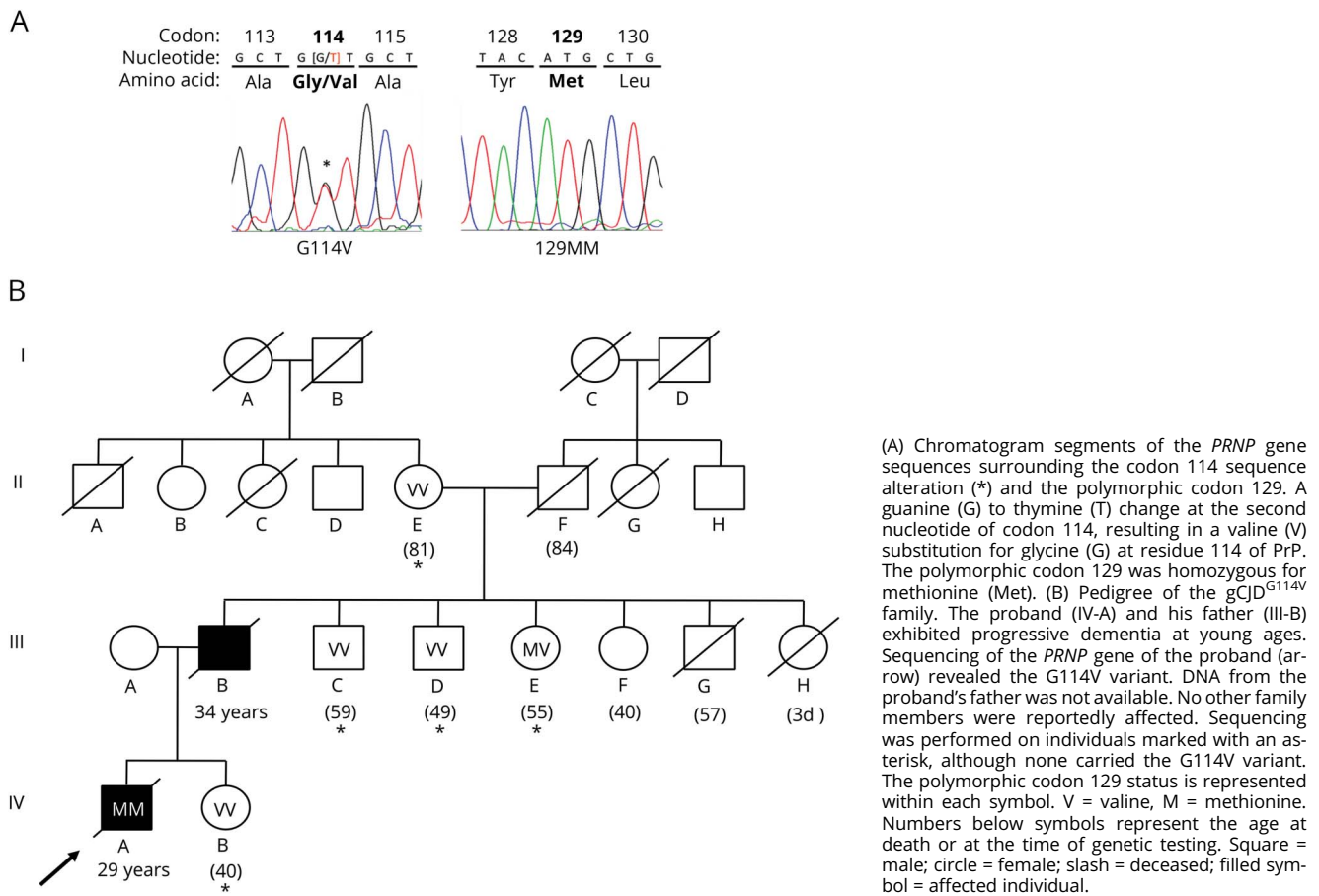
Sequencing the entire coding segment of the *PRNP* gene of the proband revealed a heterozygous thymine substitution of guanine at the second nucleotide of codon 114 (c.341G>T), resulting in a change in coding from glycine (G) to valine (V) (G114V) (figure 3A). The polymorphic codon 129, which is known to confer susceptibility to prion disease, modify disease phenotype, and influence the conformation of PrP^{Sc}, was homozygous for methionine (129MM) (figure 3). No other alterations were detected. Although no genetic information was available from the proband's father, based on the early age at disease onset and similarity of the presentation, we assumed that he carried the same *PRNP*-G114V variant. A pedigree was constructed, based on information provided by family members

Figure 2 Histopathology and immunohistochemistry of brain sections from the proband and proband's father



(A–L) Hematoxylin and eosin (H&E) staining of the proband (A–F) and proband's father (G–L). (A–D) Severe spongiform degeneration (SD) affecting frontal lobe (A) and putamen (D), and mild SD in the occipital lobe (B) and CA1 region of the hippocampus (C). (E–F) No SD affecting the midbrain (E) and cerebellum (F). (G, H, J) Severe SD affecting the frontal lobe (G), and mild SD in the parietal lobe (H) and putamen (J). (I, K–L) No SD affecting the hippocampus (I), midbrain (K), and cerebellum (L). Arrows in B, C, and J indicate SD. (M–Q) PrP immunostaining of the proband. (M and N) Diffuse PrP staining affecting the frontal lobe (M) and subiculum (N); the arrow in (N) indicates a cluster of larger PrP granules of different size. (O) Intense PrP staining at the interface between the dentate gyrus and Ammon horn (arrows); the inset depicts a high magnification of the area outlined by the dashed rectangle. (P and Q) Plaque-like PrP immunostaining in the putamen (P) and cerebellum (Q); antibody: 3F4. (R) Intense gliosis (arrow) affecting the temporal cortex; antibody: GFAP.

Figure 3 Gene sequencing and pedigree analysis



(figure 3B). The paternal grandmother (II-E) was alive at 81, although the paternal grandfather reportedly died without dementia at age 84 years and none of the father's 6 siblings, aged 40–59 years, developed a progressive neurologic disorder. A paternal uncle died of cancer at age 57 years (III-G) and an aunt died 3 days after birth (IIII). We sequenced the coding segment of the *PRNP* gene of 5 unaffected family members, including the paternal grandmother (II-E), 3 of his father's siblings (III-C, D, and E) and the proband's sister (IV-B). None carried the G114V variant, and the polymorphic codon 129 genotype was homozygous for Val (129VV) in 4 members (II-E, III-C, III-D, and IV-B) and 129MV in 1 (III-E). Since the paternal grandmother (II-E) was 129VV and the G114V change is on the 129M allele, the grandfather would be predicted to have a 129MV genotype and be a silent carrier of G114V on the 129M allele. However, surprisingly, the genotype of the proband's aunt (III-E) was 129MV with a normal 129M allele.

Typing of PrP^{Sc}

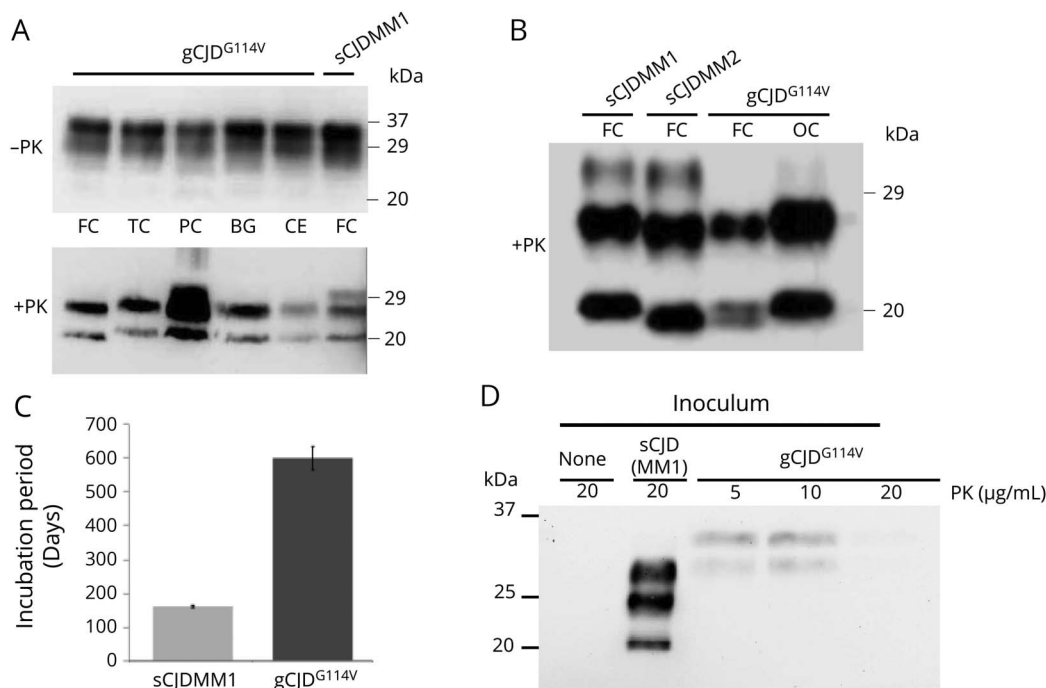
The PrP^{Sc} conformation enciphers the clinicopathologic phenotype of prion disease.^{16,18} The gel mobility of resPrP^{Sc} is an indirect measure of the PrP^{Sc} conformation. Although easily detected by WB within each brain region tested, the

level of resPrP^{Sc} varied from highest in the parietal cortex to lowest in the cerebellum (figure 4A). In contrast to the typical resPrP^{Sc} of sCJD, resPrP^{Sc} from gCJD^{G114V} lacked the diglycosylated band, exhibiting only prominent mono-glycosylated, and less prominent unglycosylated, resPrP^{Sc} bands. In addition, compared with the ~21 kDa gel mobility of unglycosylated resPrP^{Sc} from all other brain regions, initial WB of resPrP^{Sc} from the frontal lobe showed a gel mobility of ~19 kDa, matching that of PrP^{Sc} type 2 (figure 4A). Following multiple extended electrophoretic runs, a doublet was revealed, supporting the coexistence of PrP^{Sc} types 1 and 2 in the frontal cortex (figure 4B).¹⁹ These findings were independently replicated at the University of Chicago and Case Western Reserve University.

Transmission studies

Previous work shows that sequence homology between PrP^{Sc} and PrP^C at critical sites within PrP, especially at the polymorphic residue 129, is known to affect the efficiency of transmission.^{5,20} As such, we used Tg(HuPrP-129M) mice that express human PrP with Met at residue 129, to match the 129 coding of the proband. Surprisingly, after nearly 700 days following intracerebral inoculation with BH from the proband, no clinical signs of disease or histopathologic changes

Figure 4 Assessment of PrP^{Sc} type and transmissibility of gCJD^{G114V} to Tg(HuPrP) mice



(A) WB prepared from brain homogenates (BHs) of the proband and control patient with sCJDMM1 probed with mAb 3F4. Equal total protein loads compare several brain regions with a case of sCJDMM1 before (top) and after (bottom) proteinase K (PK) digestion to reveal PK-resistant PrP^{Sc} (resPrP^{Sc}). The electrophoretic profile of untreated samples from gCJD^{G114V} and sCJDMM1 appeared similar, although after digestion, all samples from the proband lacked the diglycosylated band. The parietal lobe carried the highest level of resPrP^{Sc}. (B) WB showing coexisting resPrP^{Sc} types 1 and 2 in the frontal cortex (FC; lane 3), and type 1 in the occipital cortex (OC; lane 4) of gCJD^{G114V}, compared with resPrP^{Sc} type 1 (lane 1) and type 2 (lane 2) from sCJDMM1 and sCJDMM2, respectively. (C) Survival times (days) of Tg(HuPrP-129M) mice following intracerebral inoculation of 30 µL of 1% frontal cortex BH from the gCJD^{G114V} proband compared with sCJDMM1 (n = 6 mice per group). One mouse inoculated with gCJD^{G114V} was killed 600 days after inoculation because of signs of aging, although the remainder were healthy and without symptoms after nearly 700 days when they were killed. All Tg(HuPrP-129M) mice inoculated with sCJDMM1 died with signs of prion disease (rough coat, hunched back, and unsteady gait) at 161.7 ± 4.0 days. (D) WB of representative mouse brain samples confirming the absence of resPrP^{Sc} in mice inoculated with gCJD^{G114V} compared with the high level of resPrP^{Sc} in mice inoculated with sCJDMM1.

(not shown) were evident, whereas control Tg(HuPrP-129M) mice inoculated with BH prepared from a case of sCJDMM1 yielded efficient transmission after 161.7 ± 4.0 days (figure 4C). WB prepared from inoculated mice revealed no resPrP^{Sc} from mice inoculated with gCJD^{G114V} compared with robust levels of resPrP^{Sc} type 1 in mice inoculated with sCJDMM1 (figure 4D).

Protein misfolding cyclic amplification

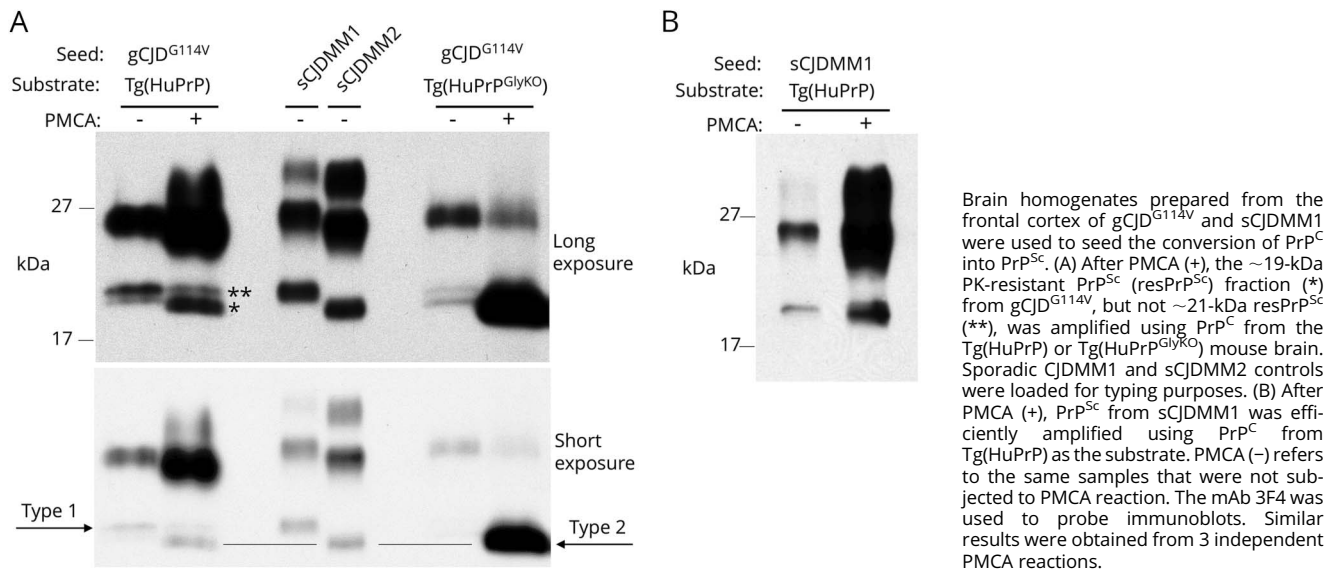
We wondered whether propagation of PrP^{Sc} from gCJD^{G114V} could be demonstrated using PMCA because this technique allows for a more controlled setting that might enhance prion propagation. BH from healthy Tg(HuPrP-129M) and Tg(HuPrP^{GlyKO}) mice was used as the substrate in separate reactions with PrP^{Sc} from the proband as the seed. The proband's resPrP^{Sc} prepared in conversion buffer and not subjected to PMCA confirmed the presence, under these conditions, of mixed PrP^{Sc} types 1 and 2 lacking the diglycosylated fraction (figure 5A). PMCA reactions using Tg(HuPrP) as substrate amplified PrP^{Sc} type 2, but not type 1. Only monoglycosylated and nonglycosylated bands were present, confirming the absence of a diglycosylated seed. Preferential PrP^{Sc} type 2 amplification was also observed using BH from Tg(HuPrP^{GlyKO}) mice

that express a mutated form of human PrP that lacks N-linked sugar chains at residues 181 and 197 (figure 5A). As the control, PrP^{Sc} from sCJDMM1, with all glycoforms, was robustly amplified using Tg(HuPrP) brain as the PrP^C substrate (figure 5B).

Discussion

We report the clinicopathologic, molecular, and transmissible properties of gCJD^{G114V} in an American-born individual of Polish descent, with no known linkage to either of the 2 previously reported families from China and Uruguay.^{8,9} Although the proband and his father had a generally similar course that included progressive dementia and aphasia, disease onset in the proband was marked by behavioral change, primarily anxiety attacks, followed by extrapyramidal features, myoclonus, and generalized ataxia. A similar course, with behavioral changes, was described for most of the 5 affected members of the Uruguayan family, although ataxia was not a feature. Ataxia was also not described in the Chinese family, although aphasia was reported. DWI imaging of our proband revealed widespread cortical and caudate hyperintensities, although CSF 14-3-3 protein was negative. A similar pattern

Figure 5 Amplification of PrP^{Sc} by protein misfolding cyclic amplification (PMCA)



of widespread DWI hyperintensity and negative CSF 14-3-3 protein was noted in the Chinese family proband, although neither of these studies were provided in the Uruguayan family report.

The early onset of our proband and his father compare well with onsets ranging from 18 to 45 years in the earlier reported families. Despite the early onset of disease, which suggests high penetrance, 45- and 61-year-old asymptomatic carriers of the G114V variant of *PRNP* were reported in the Uruguayan and Chinese families, which suggests incomplete or variable penetrance. Although our proband and his father were the only 2 affected family members, the G114V variant was not detected in other members sampled, which limits our ability to comment on penetrance. Based on the codon 129 genotypes, we suggest that the sequence alteration could have either arisen de novo in the paternal grandfather's germline or that a nonpaternity event skewed the genetics of this pedigree. However, the typically early onset and the lack of disease in previous generations raise questions whether anticipation or, more likely, other genetic or environmental factors play a significant role in disease manifestation linked to this genetic variant.

The pathogenicity of the G114V variant is supported by its position within the highly conserved palindromic segment of PrP (113-AGAAAAGA-120) that features directly in the formation of PrP^{Sc} and the PrP^{Sc}-PrP^C complex that leads to propagation of PrP^{Sc}.²¹ Although the G114V and A117V variants lie within this palindrome, 3 other pathogenic alterations (G131V, S132I, and A133V) lie slightly downstream, but still within the hydrophobic core that extends from residue 113 to 134. Curiously, each of these promotes a Gerstmann-Sträussler-Scheinker (GSS) disease

phenotype, defined by the presence of multicentric PrP amyloid plaques isolated to the cerebellum or diffusely distributed throughout the cortex and deep nuclei.²²⁻²⁷ Globular PrP deposits were present within the cerebellum and putamen of the proband, but these were sparse and were not detected in his father or the 2 previously reported gCJD^{G114V} families.^{8,9}

The gel mobility of resPrP^{Sc} is an indirect measure of PrP^{Sc} conformation, which differs among the major subtypes of prion disease.^{2,28} The gel migration pattern of CJD-derived resPrP^{Sc} typically includes 3 glycoforms that range from ~19 or 21 to 30 kDa, whereas GSS-associated resPrP^{Sc} has a single nonglycosylated band of 7-16 kDa, representing N- and C-terminally cleaved PrP^{Sc}. The resPrP^{Sc} associated with A133V has not been reported, but that from A117V,^{29,30} S132I,²² and G131V²⁴ conforms to the GSS pattern. That from our proband migrates more characteristically as CJD, despite the absence of the diglycosylated fraction. Of interest, a similar pattern has been reported with the T183A,³¹ V180I,³² and P105S¹⁰ variants and in a single case of sCJD.³³ Although the sequence changes at residues 180 and 183 could directly interfere with nearby N-linked glycosylation sites at residue 181, the distal location of residues 105 and 114, and the occurrence of this resPrP^{Sc} type in a sCJD case, suggests that the conformation of this rare PrP^{Sc} type favors selection of the unglycosylated and monoglycosylated PrP^{Sc} isoforms. Although we also found a mixture of ~19- and ~21-kDa resPrP^{Sc} in our proband, this feature has been reported in as many as ~40% of sCJD cases with the 129MM genotype¹⁹ and in rare cases of gCJD^{E200K}³⁴ and gCJD^{D178N}.³⁵ Overall, the clinicopathologic and molecular typing characteristics best suggest that the *PRNP*-G114V variant should be categorized as a CJD subtype.

The lack of transmission of gCJD^{G114V} to TgHuPrP mice implies that the sequence change at residue 114 introduces a barrier to transmission. Efficient prion transmission has been shown to depend on the balance of two critical determinants: (1) sequence homology between PrP^{Sc} and PrP^C at key sites of association within the PrP^{Sc}-PrP^C interface and (2) the ability of PrP^C to acquire the conformation of PrP^{Sc}. We can speculate that the sequence alteration at residue 114 that sits within the highly conserved palindrome represents a mismatch at an association site within the PrP^{Sc}-PrP^C interface or the conformation of PrP^{Sc} induced by the G114V variant falls outside the conformational repertoire that PrP^C in TgHuPrP mice can adopt. Although data are limited regarding the transmissibility of disease resulting from other variants within the palindromic region, we have not had success transmitting GSS^{A117V} to Tg(HuPrP) mice (unpublished observations). Whether this relates to a universal feature of GSS to poorly transmit disease compared with CJD^{36,37} or the sequence mismatch at residue 117, was addressed by 1 group that successfully transmitted GSS^{A117V} to a Tg mouse expressing the homologous sequence change.³⁸ In addition, a more recent study found that bank voles are susceptible to GSS prions, suggesting that the sequence of bank vole PrP^C can adopt the conformation of PrP^{Sc} in GSS^{A117V} despite the absence of homology at residue 117 between PrP^{Sc} and PrP^C.³⁹ Thus, the conformation of PrP^{Sc} linked to the PRNP-G114V variant may, in fact, be the principal barrier to transmission. The finding that PMCA amplification of this conformation was possible suggests that conditions of this artificial system are more favorable for the PrP^{Sc}-PrP^C association that leads to propagation of PrP^{Sc}. However, despite the partially positive results, a conformational barrier to prion propagation was still evident, based on the selective amplification of the 19-kDa resPrP^{Sc} fraction. Recent work suggests that in the presence of 2 conformational subtypes of PrP^{Sc}, PMCA favors amplification of the least stable conformer,¹⁴ which is suggested to be the 19-kDa PrP^{Sc} fraction in this case, based on its limited presence within the frontal lobes, compared with the widespread presence of the 21-kDa conformer.

Our findings demonstrate that the G114V variant of PRNP promotes a CJD clinicopathologic phenotype linked to an atypical PrP^{Sc} conformation that lacks the diglycosylated fraction and is poorly transmissible to Tg(HuPrP) mice. Although the G114V variant of PRNP appears to be associated with variable penetrance that is not yet well characterized, its location within the highly conserved palindromic segment of the hydrophobic core of PrP and the associated atypical conformation of PrP^{Sc} are likely to contribute to the unique properties of gCJD^{G114V} prions that we observed. Overall, these findings highlight the importance of this residue and the palindrome in prion conformation and propagation and as a potential target of therapy.

Author contributions

I. Cali: histologic preparations, data interpretation, and generation of figures and text for manuscript preparation. K. Qin:

preparation of Western blots, interpretation of data, and assistance with text preparation. F. Mikhail: patient data acquisition, preparation of figures, and manuscript writing. A. Solanki: breeding and maintenance of mice and inoculation and monitoring of mice for transmission studies. M.C. Martinez: performed PMCA. L. Zhao: mouse screening and gene sequencing of family members and transgenic mice. C. Gregory: preparation of Western blots, collection of blood samples from subjects, preparation of inoculums, and inoculation of mice for transmission studies. P. Gambetti: histologic studies, data interpretation, and manuscript preparation. E. Norstorm: preparation of figures, data assessment, and manuscript writing. J.A. Mastrianni: design of the study, interpretation of data, and manuscript preparation. B. Appleby: tissue samples and personnel resources.

Study funding

This work was supported by an endowment from the Brain Research Foundation (J.A.M.), NIH P01AI106705, NIH 5R01NS083687, and Charles S. Britton Fund (P.G.); The National Prion Disease Pathology Surveillance Center.

Disclosure

I. Cali serves as an editorial board member of the *World Journal of Neurology*, *BioMed International*, and the *Asian Journal of Neuroscience*. K. Qin reports no disclosures. F. Mikhail has received research funding from the NRSA T32 Ruth Kirschstein Training Grant. C. Gregory, A. Solanki, M.C. Martinez, and L. Zhao report no disclosures. P. Gambetti has served on the scientific advisory board of Ferring Pharmaceuticals; holds a patent for Sant Cruz BioTechnology (A2006-03237); and has received research funding from the NIH. E. Norstrom reports no disclosures. J.A. Mastrianni has served on the scientific advisory board of the Alzheimer's Association; has consulted for CVS Caremark and the Federal Trade Commission; has received commercial research funding from Eli Lilly and the CMS and Alzheimer's Association; and has received research funding from the Brain Research Foundation. Full disclosure form information provided by the authors is available with the full text of this article at Neurology.org/NG.

Received February 9, 2018. Accepted in final form May 14, 2018.

References

1. Prusiner SB. Prions (Les Prix Nobel Lecture). In: Frängsmyr T, editor. *Les Prix Nobel*. Stockholm: Almqvist & Wiksell International; 1998:268–323.
2. Brown K, Mastrianni JA. The prion diseases. *J Geriatr Psychiatry Neurol* 2010;23: 277–298.
3. Parchi P, Castellani R, Capellari S, et al. Molecular basis of phenotypic variability in sporadic Creutzfeldt-Jakob disease. *Ann Neurol* 1996;39:767–778.
4. Watts JC, Prusiner SB. Mouse models for studying the formation and propagation of prions. *J Biol Chem* 2014;289:19841–19849.
5. Mallik S, Yang W, Norstrom EM, Mastrianni JA. Live cell fluorescence resonance energy transfer predicts an altered molecular association of heterologous PrP^{Sc} with PrP^C. *J Biol Chem* 2010;285:8967–8975.
6. Castilla J, Gonzalez-Romero D, Saa P, Morales R, De Castro J, Soto C. Crossing the species barrier by PrP(Sc) replication in vitro generates unique infectious prions. *Cell* 2008;134:757–768.
7. Jones M, Peden AH, Head MW, Ironside JW. The application of in vitro cell-free conversion systems to human prion diseases. *Acta Neuropathol* 2011;121: 135–143.
8. Ye J, Han J, Shi Q, et al. Human prion disease with a G114V mutation and epidemiological studies in a Chinese family: a case series. *J Med Case Rep* 2008;2: 331.

9. Rodriguez MM, Peoc'h K, Haik S, et al. A novel mutation (G114V) in the prion protein gene in a family with inherited prion disease. *Neurology* 2005;64:1455–1457.
10. Tunnell E, Wollman R, Mallik S, Cortes CJ, Dearmond SJ, Mastrianni JA. A novel PRNP-P105S mutation associated with atypical prion disease and a rare PrPSc conformation. *Neurology* 2008;71:1431–1438.
11. Kascsak RJ, Rubenstein R, Merz PA, et al. Mouse polyclonal and monoclonal antibody to scrapie-associated fibril proteins. *J Virol* 1987;61:3688–3693.
12. Zou WQ, Puoti G, Xiao X, et al. Variably protease-sensitive prionopathy: a new sporadic disease of the prion protein. *Ann Neurol* 2010;68:162–172.
13. Telling GC, Scott M, Mastrianni J, et al. Prion propagation in mice expressing human and chimeric PrP transgenes implicates the interaction of cellular PrP with another protein. *Cell* 1995;83:79–90.
14. Haldiman T, Kim C, Cohen Y, et al. Co-existence of distinct prion types enables conformational evolution of human PrPSc by competitive selection. *J Biol Chem* 2013;288:29846–29861.
15. Castilla J, Saa P, Morales R, Abid K, Maundrell K, Soto C. Protein misfolding cyclic amplification for diagnosis and prion propagation studies. *Methods Enzymol* 2006;412:3–21.
16. Mastrianni JA, Nixon R, Layzer R, et al. Prion protein conformation in a patient with sporadic fatal insomnia. *N Engl J Med* 1999;340:1630–1638.
17. Folstein M, Folstein S, McHugh PR. “Mini-mental status”: a practical method for grading the cognitive state of patients for the clinician. *J Psychiatr Res* 1975;12:189–198.
18. Telling GC, Parchi P, DeArmond SJ, et al. Evidence for the conformation of the pathologic isoform of the prion protein enciphering and propagating prion diversity. *Science* 1996;274:2079–2082.
19. Cali I, Castellani R, Alshekhlee A, et al. Co-existence of scrapie prion protein types 1 and 2 in sporadic Creutzfeldt-Jakob disease: its effect on the phenotype and prion-type characteristics. *Brain* 2009;132:2643–2658.
20. Wadsworth JD, Asante EA, Desbruslais M, et al. Human prion protein with valine 129 prevents expression of variant CJD phenotype. *Science* 2004;306:1793–1796.
21. Norstrom EM, Mastrianni JA. The AGAAAAGA palindrome in PrP is required to generate a productive PrPSc-PrPC complex that leads to prion propagation. *J Biol Chem* 2005;280:27236–27243.
22. Hilton DA, Head MW, Singh VK, Bishop M, Ironside JW. Familial prion disease with a novel serine to isoleucine mutation at codon 132 of prion protein gene (PRNP). *Neuropathol Appl Neurobiol* 2009;35:111–115.
23. Panegyres PK, Toufexis K, Kakulas BA, et al. A new PRNP mutation (G131V) associated with Gerstmann-Straussler-Scheinker disease. *Arch Neurol* 2001;58:1899–1902.
24. Jansen C, Parchi P, Capellari S, et al. A second case of Gerstmann-Straussler-Scheinker disease linked to the G131V mutation in the prion protein gene in a Dutch patient. *J Neuropathol Exp Neurol* 2011;70:698–702.
25. Kovacs GG, Ertsey C, Majtenyi C, et al. Inherited prion disease with A117V mutation of the prion protein gene: a novel Hungarian family. *J Neurol Neurosurg Psychiatry* 2001;70:802–805.
26. Mastrianni JA, Curtis MT, Oberholtzer JC, et al. Prion disease (PrP-A117V) presenting with ataxia instead of dementia. *Neurology* 1995;45:2042–2050.
27. Mohr M, Tranchant C, Steinmetz G, Floquet J, Grignon Y, Warter JM. Gerstmann-Straussler-Scheinker disease and the French-Alsatian A117V variant. *Clin Exp Pathol* 1999;47:161–175.
28. Parchi P, Giese A, Capellari S, et al. Classification of sporadic Creutzfeldt-Jakob disease based on molecular and phenotypic analysis of 300 subjects. *Ann Neurol* 1999;46:224–233.
29. Yang W, Cook J, Rassbach B, Lemus A, DeArmond SJ, Mastrianni JA. A new transgenic mouse model of Gerstmann-Straussler-Scheinker syndrome caused by the A117V mutation of PRNP. *J Neurosci* 2009;29:10072–10080.
30. Tagliavini F, Lievens PM, Tranchant C, et al. A 7-kDa prion protein (PrP) fragment, an integral component of the PrP region required for infectivity, is the major amyloid protein in Gerstmann-Straussler-Scheinker disease A117V. *J Biol Chem* 2001;276:6009–6015.
31. Grasbon-Frodl E, Lorenz H, Mann U, Nitsch RM, Windl O, Kretzschmar HA. Loss of glycosylation associated with the T183A mutation in human prion disease. *Acta Neuropathol (Berl)* 2004;108:476–484.
32. Chasseigneaux S, Haik S, Laffont-Proust I, et al. V180I mutation of the prion protein gene associated with atypical PrPSc glycosylation. *Neurosci Lett* 2006;408:165–169.
33. Zanusso G, Polo A, Farinazzo A, et al. Novel prion protein conformation and glyco-type in Creutzfeldt-Jakob disease. *Arch Neurol* 2007;64:595–599.
34. Kovacs GG, Seguin J, Quadrio I, et al. Genetic Creutzfeldt-Jakob disease associated with the E200K mutation: characterization of a complex proteinopathy. *Acta Neuropathol* 2011;121:39–57.
35. Haik S, Peoc'h K, Brandel JP, et al. Striking PrPSc heterogeneity in inherited prion diseases with the D178N mutation. *Ann Neurol* 2004;56:909–910. author reply 10–11.
36. Brown P, Gibbs CJ Jr, Rodgers-Johnson P, et al. Human spongiform encephalopathy: the National Institutes of Health series of 300 cases of experimentally transmitted disease. *Ann Neurol* 1994;35:513–529.
37. Tateishi J, Kitamoto T, Hoque MZ, Furukawa H. Experimental transmission of Creutzfeldt-Jakob disease and related diseases to rodents. *Neurology* 1996;46:532–537.
38. Asante EA, Linehan JM, Smidak M, et al. Inherited prion disease A117V is not simply a proteinopathy but produces prions transmissible to transgenic mice expressing homologous prion protein. *PLoS Pathog* 2013;9:e1003643.
39. Pirisinu L, Di Bari MA, D'Agostino C, et al. Gerstmann-Straussler-Scheinker disease subtypes efficiently transmit in bank voles as genuine prion diseases. *Sci Rep* 2016;6:20443.

Neurology[®] Genetics

Impaired transmissibility of atypical prions from genetic CJD^{G114V}

Ignazio Cali, Fadi Mikhail, Kefeng Qin, et al.

Neurol Genet 2018;4;

DOI 10.1212/NXG.0000000000000253

This information is current as of August 7, 2018

Updated Information & Services	including high resolution figures, can be found at: http://ng.neurology.org/content/4/4/e253.full.html
References	This article cites 38 articles, 10 of which you can access for free at: http://ng.neurology.org/content/4/4/e253.full.html##ref-list-1
Citations	This article has been cited by 1 HighWire-hosted articles: http://ng.neurology.org/content/4/4/e253.full.html##otherarticles
Subspecialty Collections	This article, along with others on similar topics, appears in the following collection(s): All Clinical Neurology http://ng.neurology.org/cgi/collection/all_clinical_neurology All Genetics http://ng.neurology.org/cgi/collection/all_genetics Prion disease; see Infections/prion http://ng.neurology.org/cgi/collection/prion_disease
Permissions & Licensing	Information about reproducing this article in parts (figures, tables) or in its entirety can be found online at: http://ng.neurology.org/misc/about.xhtml#permissions
Reprints	Information about ordering reprints can be found online: http://ng.neurology.org/misc/addir.xhtml#reprintsus

Neurol Genet is an official journal of the American Academy of Neurology. Published since April 2015, it is an open-access, online-only, continuous publication journal. Copyright © 2018 The Author(s). Published by Wolters Kluwer Health, Inc. on behalf of the American Academy of Neurology. All rights reserved. Online ISSN: 2376-7839.

